EUROPEAN ORGANIZATION FOR NUCLEAR RESEARCH

CERN-PPE/91-188
9 OCTOBER 1991

Recent Results from the Crystal Barrel Experiment

THE CRYSTAL BARREL COLLABORATION

C Amsler[13], I. Augustin[6], C. A. Baker[11], B. M. Barnett[13], C. J. Batty[11], R. Beckmann[5], K. Beuchert[2], P. Birien[1], J. Bistirlich[1], P. Blüm[6] R. Bossingham[1], H. Bossy[1], K. Braune[10], D. V. Bugg[7], M. Burchell[4], T. Case[1], K. M. Crowe[1], W. Dünnweber[10], D. Engelhardt[6], M. Faessler[10], C. Felix[10], G. Folger[10], R. Haddock[8], F.H. Heinsius[5], N. P. Hessey[11], P. Illinger[10], D. Jamnik[10], H. Kalinowsky[9], B. Kämmle[5], T. Kiel[5], E. Klempt[9], H. Koch[2], K. Königsmann[10], M. Kunze[2], R. Landua[4], H. Matthäy[2], M. Merkel[9],J.P. Merlo[9], C. A. Meyer[13], U. Meyer-Berkhout[10], L. Montanet[4],A. Noble[13], K. Peters[9], G. Pinter[3], S. Ravndal[2], A. Sanjari[7],E. Schäfer[9], B. Schmid[13],C. Strassburger[9], U. Strohbusch[5], M. Suffert[12], D. Urner[13], D. Walther[2], U. Wiedner[5], N. Winter[6], J. Zoll[4], C. Zupancic[10]

[1]*University of California Berkeley / LBL*
[2]*University of Bochum*
[3]*Academy of Science Budapest*
[4]*CERN*
[5]*University of Hamburg*
[6]*University of Karlsruhe*
[7]*Queen Mary and Westfield College London*
[8]*University of California Los Angeles*
[9]*University of Mainz*
[10]*University of München*
[11]*Rutherford Appleton Laboratory Chilton*
[12]*Centre de Recherches Nucleaires Strasbourg*
[13]*University of Zurich*

Invited talk given at NAN 91, Moscow, July 8-11
to be published in the proceedings

ABSTRACT

The Crystal Barrel experiment has been constructed and installed at the Low Energy Antiproton Ring (LEAR) at CERN. It has been fully operational since late 1989. In this talk, recent results of meson spectroscopy in $\bar{p}p$-annihilations are presented. The main emphasis is on all-neutral annihilations, the study of the strange quark content of the proton, and the investigation of the decay mode of η particles. A 2^{++} resonance decaying into $\pi^\circ\pi^\circ$ at a mass of 1515 ± 10 MeV with a width of 120 ± 10 MeV has been seen in a $3\pi^\circ$ final state.

Introduction and Motivation

The study of $\bar{p}p$ annihilation has been underway for the past thirty years. Several bubble chamber experiments at CERN and BNL first investigated this topic [1,2]. In the 1980's LEAR came into operation, providing an intensive and extremely pure source of antiprotons. The first generation of LEAR experiments produced interesting new results. Nevertheless, none of these experiments was able to investigate the 60% of annihilation channels which contain more than one neutral particle in the final state. This led to the formation of the Crystal Barrel collaboration, composed of over 40 scientists from 13 different institutions. Its aim was the construction of a detector which covers almost 4 π solid angle and detects neutral particles as effectively as charged particles.

$\bar{p}p$ annihilations are a very rich source of ordinary $q\bar{q}$ mesons such as π,η, and ω. The formation of exotic particles like multiple (>2) quark states, glueballs or hybrids is likely to happen in an extended quark-gluon system like protonium. Exotic particles are particularly expected to exist in all-neutral final states and in final states with more than one neutral particle. The search for these exotics is the main motivation for the Crystal Barrel experiment.

With theories of hadronic interaction getting better and better in the past years, it has become clear that the quality of existing data from old experiments is not at all sufficient. Certain nonexotic channels have still not been investigated. Crystal Barrel, a 4π detector with high precision in detection of neutral and charged particles, is very well suited to such research and its data should help to check Quantum Chromodynamics (QCD) in the low energy region, where it is very little tested so far.

The first round of data-taking with the Crystal Barrel Detector was dedicated to experiments with antiprotons stopping in a liquid hydrogen target. So far, almost 30 million annihilations have been recorded.

The Detector

Figure 1 shows an overview of the detector setup. The detector is located inside a magnet that produces a field of 1.5T. Antiprotons enter the detector from the left side with a momentum of 0.2 GeV/c. They pass a beam-defining scintillator and a silicon counter just in front of the target. This silicon counter consists of four segments, each 3 x 3 $mm^2$and 200 μm thick. The counter is located 36 mm in front of the entrance window of the liquid hydrogen target and is used to optimize the focus of the beam into the target. It also gives the main trigger signal for the readout of the individual subcomponents of the detector.

The two multiwire proportional wire chambers (PWC1 and PWC2) provide fast information of the charged multiplicity of the annihilation event. They give as well additional information on the r/ϕ coordinates for charged particles close to the annihilation point in the target. The sense wires run parallel to the beam axis at radii of 25.5 and 43 mm, respectively. The spacing between the sense wires is 1.8 mm, with 90 sense wires for the inner chamber and 150 sense wires for the outer chamber. The sense wire thickness is 15 μm. The gas mixture consists of 69.5% argon, 30% ethane and 0.5% freon. The operational high voltage is 2500 V. The materials of the chambers are chosen to minimize the multiple scattering and the radiation length. The total thickness of both chambers is 2.2×10^{-3} radiation lengths. The outermost diameters of PWC1 and PWC2 cover 99% and 97% of the 4π solid angle. The readout of the PWCs is done with the PCOS III system of LeCroy, which

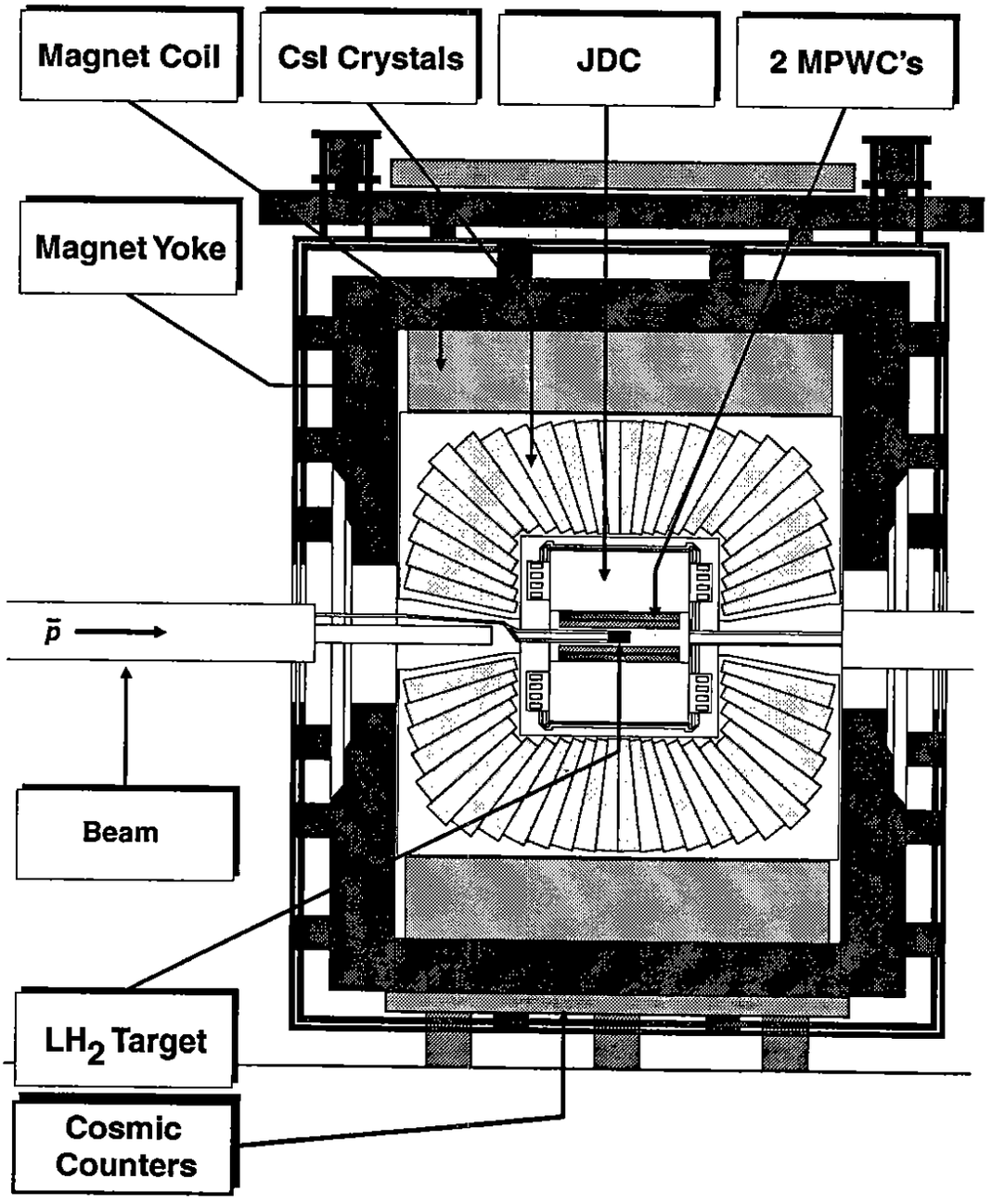

Fig. 1: The Crystal Barrel Detector

provides fast signals on wires fired in the chamber. Adjacent hits are called clusters. The electronics connected to the readout system then determines the number of charged particle hits in the chamber.

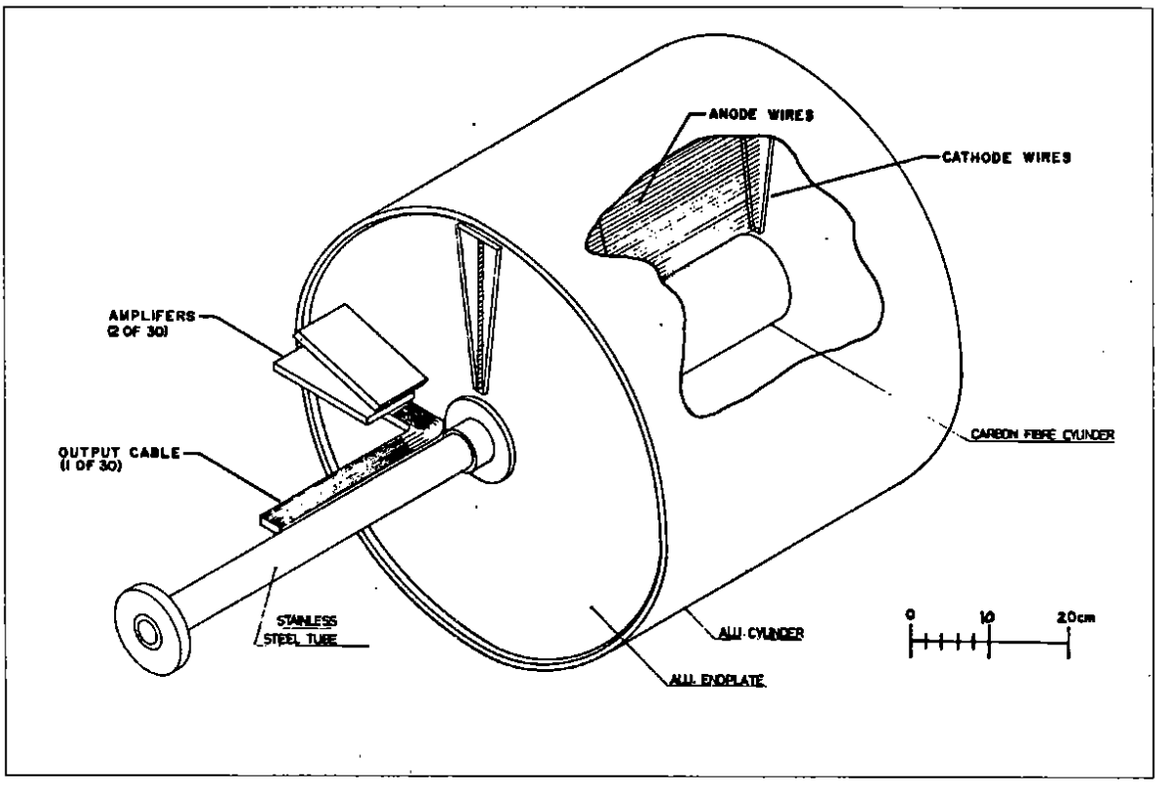

Fig. 2: The Jet Drift Chamber

The proportional wire chambers are located inside a cylindrical Jet Drift Chamber (JDC). Figure 2 shows a simplified diagram of the JDC, which is divided into 30 drift cells or sectors of the kind shown in figure 3. Each sector has two preamplifier cards and 23 signal channels (corresponding to 23 layers of sense wires), which are read out on both sides of the chamber to provide information about the z-vertex with charge division.

This arrangement allows for both short drift times and enough ionization to give a separation of kaons and pions by dE/dx. The sense wires are staggered ±200 μm to solve the problem of left/right ambiguity within a drift cell. The gas gain is mainly determined by the high voltage of the

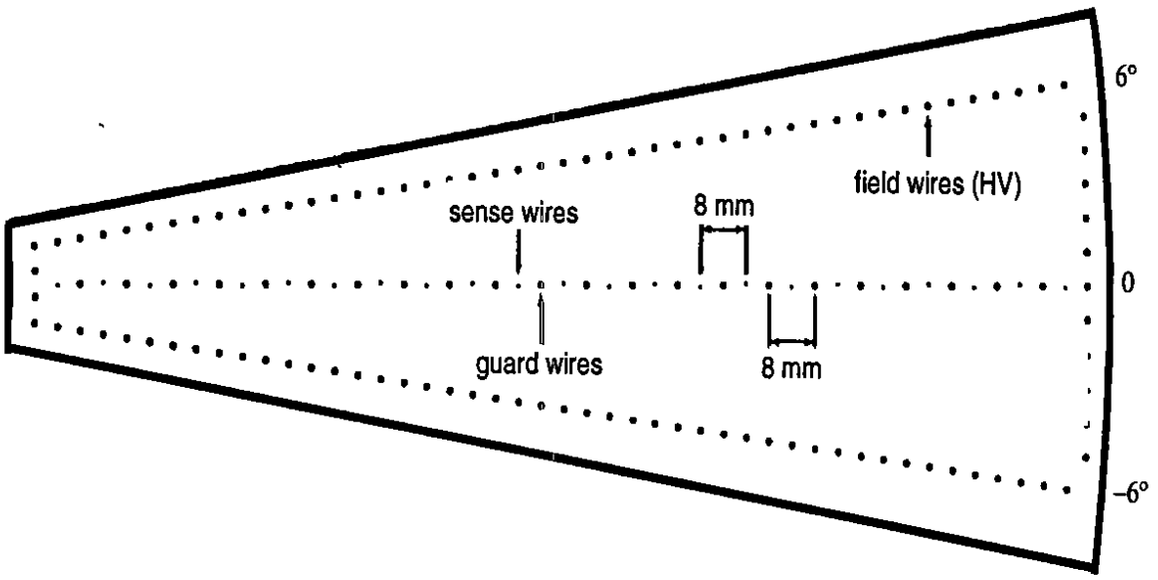

Fig. 3 Sector of the Jet Drift Chamber

guard wires located between the sense wires. With the help of the GARFIELD drift chamber program [3], the high voltage was optimized and chosen so that it provides a fairly homogeneous drift field of 1100 V/cm in the chamber. The gas mixture is of the so-called "slow type," to keep the Lorentz angle small. We use a mixture of 90% CO_2 and 10% isobutane (C_4H_{10}). The measured drift velocity is 9.2 μm/ns at a temperature of 25°C. The composition of the gas and its temperature are constantly monitored and regulated, while pressure (which also influences the drift velocity) is only monitored. In addition, a small drift chamber that runs with the output gas of the JDC measures and calibrates the drift velocity. The dimensions of the JDC are very compact: 535 mm long and 535 mm in diameter. The compact design minimizes the number of crystals needed for the electromagnetic calorimeter.

The preamplifiers for each sector are directly mounted at the endplates of the JDC. They produce differential output signals that are picked up by receiver cards located at the readout electronics. Each of the 1380 signals (690 sense wires read out on both sides) is digitized by a Flash ADC module every 10 ns, with a maximum allowed drift time of 2.56 μs for the inner layers and 10 μs for the four outermost layers. The six-bit nonlinear resolution of the Flash ADC results in an effective resolution of 8 bits.

The JDC is responsible for the detection of charged particles, while the electromagenetic calorimeter can also detect neutral particles with the use of its 1380 individual crystals (one of which is shown below in figure 4).

The material used for these crystals is thallium-doped cesium iodide, which acts as a scintillator similar to NaI but is less hygroscopic and has a shorter radiation length. The crystals are arranged as a barrel – hence the experiment's name – with each crystal pointing to the center. The crystals thus cover an azimuthal angle of almost 4π and polar angles from 12° to 168°. Each crystal's size covers 6° in both directions, except at polar angles $\theta < 30°$ and $\theta > 150°$, where each covers 12°.

The whole arrangement is designed to provide high efficiency photon detection with good energy and spatial resolution in the energy range between 10 MeV and 2000 MeV. The light emitted by

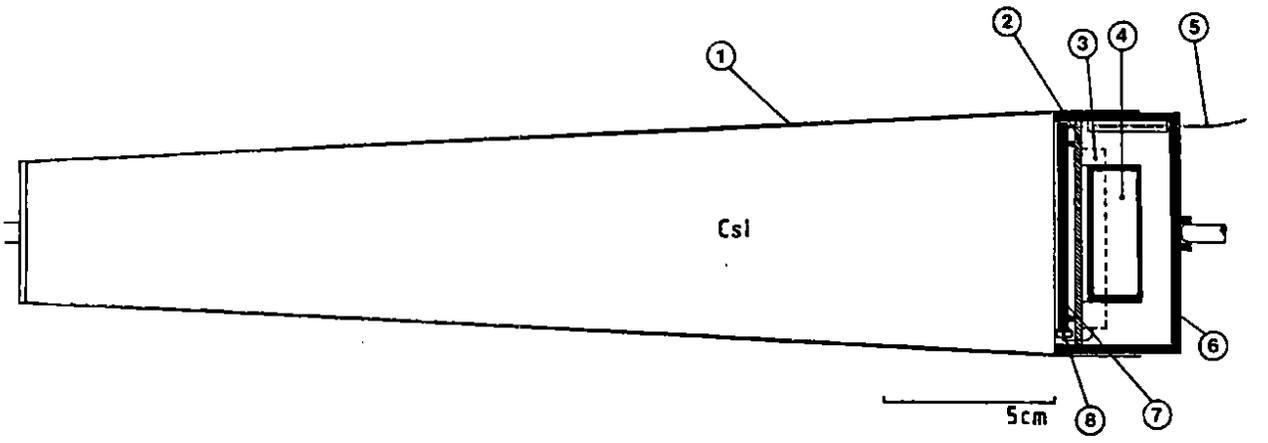

1 Titanium 0.1 mm
2 Printed Circuit Board
3 Filter for Bias and Power supplies
4 Charge-sensitive Preamplifier
5 Lightguide
6 Brass Shielding
7 Wavelength Shifter
8 Photodiode

Fig. 4: CsI-Crystal with Preamplifier (schematic)

CsI peaks around 550 nm, and each individual crystal was checked for its homogeneity in light output over the whole length. The readout of the crystals is done with photodiodes, because in a strong magnetic field readouts with photomultipliers are not possible. To match better the light emitting area of the crystal to the sensitive area of the photodiode, we placed a wavelength shifter between the two. The wavelength shifter itself has three of its four lateral sides painted with a white diffuser to increase the light collection efficiency of the photodiode glued to the fourth side.

Attached to each photodiode there is a preamplifier mounted directly on each individual crystal. The readout system for the signals coming out of the preamplifiers consists of a main shaper amplifier, a discriminator and 2 ADC types for each crystal. One of the ADCs covers the full energy range (0 - 2000 MeV) with a resolution of 1 MeV/channel, while the other has a limited energy range of max. 400 MeV but excellent resolution of 0.1 MeV/channel. The readout electronics are designed to work with a 6 μs-wide gate. We repeat the calibration for each crystal before every run period, using γ's from the π^0 decay.

There are several trigger levels in the Crystal Barrel experiment. The simplest trigger is called "minimum bias" and is started when an antiproton passes through the silicon counters. To be selective on charged multiplicities we use the PWC and 6 layers of the JDC, which are connected to a multiplicity logic. At this level one can, for example, run triggers with all-neutral particles in the final state. At the same trigger level it is also possible to select cluster multiplicities in the crystal matrix. The most sophisticated trigger of our experiment is a software trigger [4]. This software trigger allows online the selection of final states with a required number of selected neutral particles, such as π,η.

The whole experiment is controlled by several microprocessors. A Macintosh computer acts as the "human interface."

Results

The results which will be presented below can be divided into three topics:
- the search for exotic particles in all-neutral final states,
- investigations related to the question of the strangeness content of the proton, and
- the study of decay modes of η particles.

All-neutral annihilations

Until now, the Crystal Barrel experiment has recorded approximately 30 million events with anti-protons stopping in liquid hydrogen. The results presented are based on 2 million of the 17 million all-neutral final states recorded. The off-line preselection criteria require that no charged particles be seen by the PWCs or the JDC and that there be an energy deposit of at least 20 MeV in one isolated or in several neighbouring crystals. Furthermore, the approximate energy and momentum conservation must be satisfied with the sum of all momenta below 200 MeV/c and the sum of the total measured energy between 1675 MeV and 2075 MeV. The data passing these tests were then scanned for 6γ events. This includes the final states of $\pi^\circ\pi^\circ\pi^\circ$, $\pi^\circ\pi^\circ\eta$ and $\pi^\circ\eta\eta$.

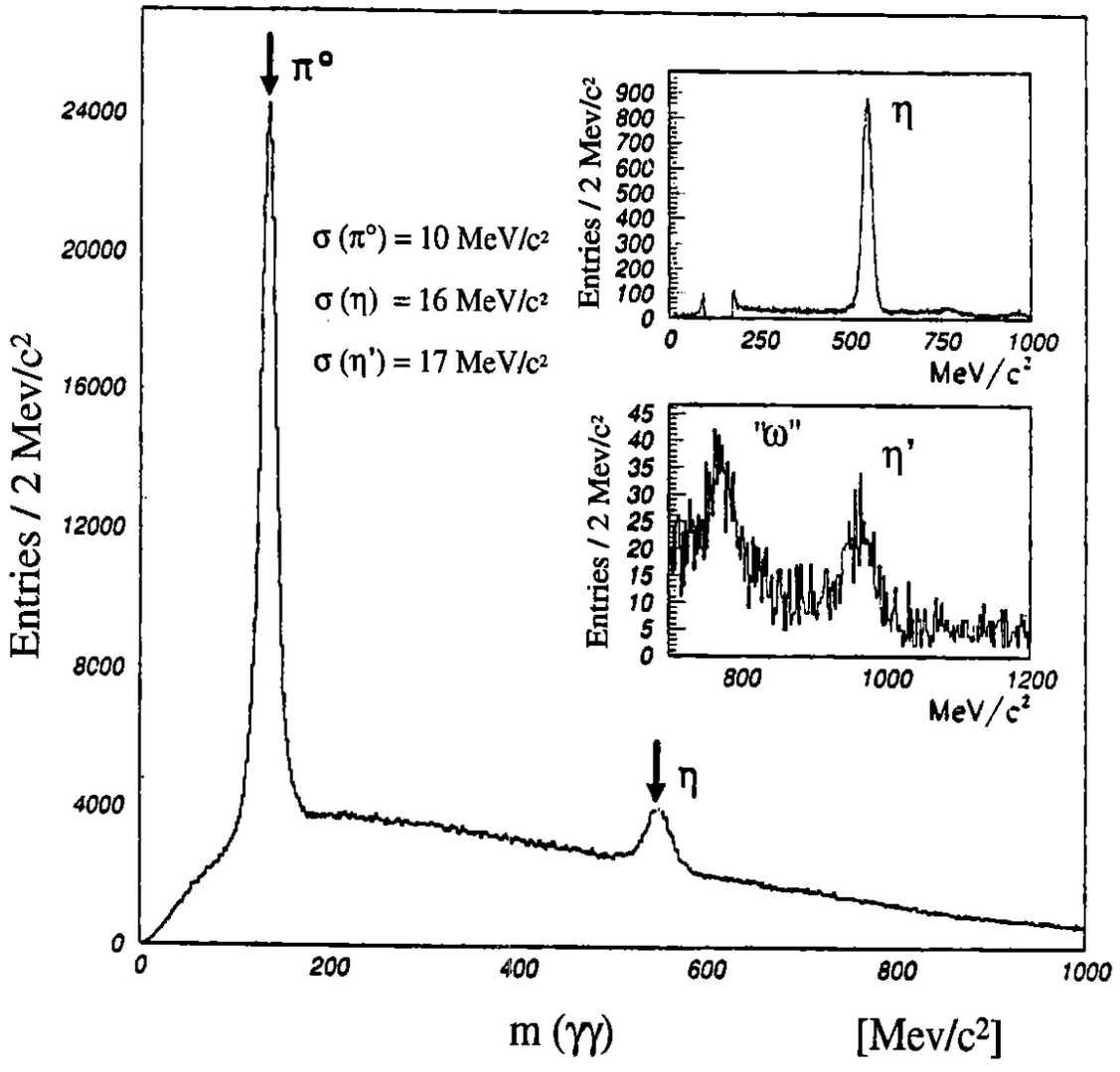

Fig. 5: Invariant 6 photon mass spectrum

The quality of the data can be seen in figure 5, which shows the invariant 6γ spectrum extracted from the six-photon sample. Because there are several possibilities for combining two photons, there are 15 entries per event. Clear π° and η peaks appear. In the upper inset only the $\gamma\gamma$ mass combinations which do not contribute to the π° mass window are shown. In the lower inset the combinations leading to an η are also taken out. This procedure reduces the combinatorial background and the η and η' signals become more apparent. The peak in the lower inset around 770 MeV shows a signal from $\pi^\circ\pi^\circ\omega$ events with the ω decaying into $\pi^\circ\gamma$. Our detector misses one very low energy γ.

First results for the channel $\bar{p}p \rightarrow \pi^\circ\pi^\circ\pi^\circ$ have been published recently [5]. 7 C fits were applied to select 3 π° events out of the 6γ data sample. The other hypotheses allowed were $\bar{p}p \rightarrow \pi^\circ\pi^\circ\eta$, $\bar{p}p \rightarrow \pi^\circ\eta\eta$ and $\bar{p}p \rightarrow \eta\eta\eta$. After the application of all the selection criteria mentioned above, the probability of non-3π° events – which form the background of the 3π° Dalitz plot – is far below 1%. The global efficiency is nearly uniform over the whole phase space.

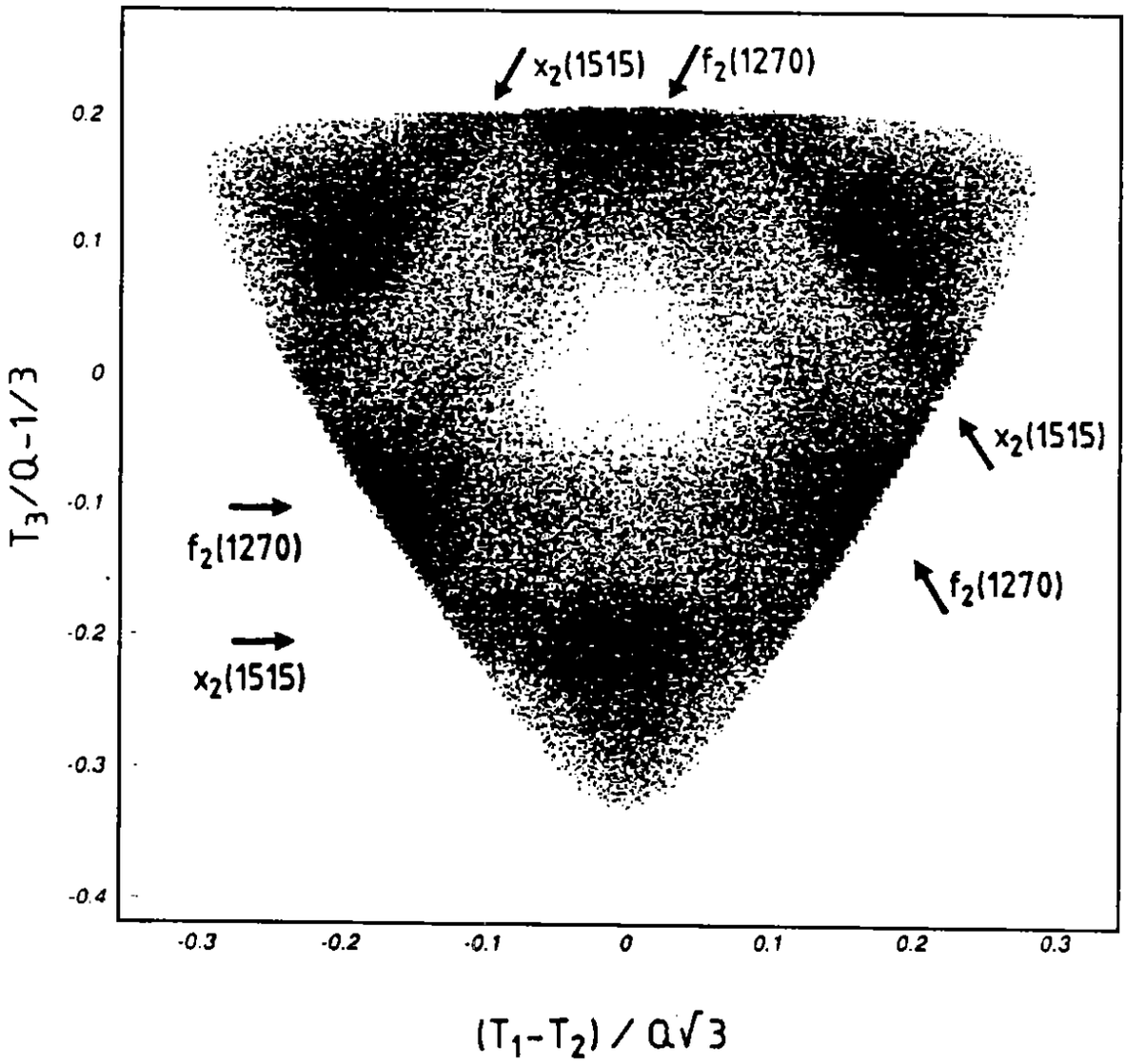

Fig. 6: 3 π° Dalitz plot in symmetrical presentation

In the 3π° Dalitz plot in figure 6, each event is plotted 6 times, once in each of the 6 sextants. The most important result is the observation of a resonance around 1520 MeV. The partial wave analysis of this Dalitz plot gives the following values for this resonance:

$M_{X2} = 1515 \pm 10$ MeV, $\Gamma = 120 \pm 10$ MeV, $J^{pc} = 2^{++}$

This resonance represents 26% of the $3\pi^\circ$ Dalitz plot (9.5% from $^1S_0$, 8% from $^3P_1$ and 8.8% from $^3P_2$ initial state). We cannot determine the isospin from this result alone, but we identify the X_2 with either the $J^P = 2^+$resonance observed by May et al. [6] at 1565 MeV (P-state annihilation) or the isoscalar two pion resonance postulated by Gray et al. [7] at 1527 MeV. Therefore the isospin must be 0. The nature of the X_2 is unknown, but it cannot be identified with the well-established f_2' at 1525 MeV because we do not observe a large decay mode into kaons reported for this resonance.

For the channel $\pi^\circ\pi^\circ\eta$ the Dalitz plot (fig. 7) contains 20,000 entries. Each event is plotted twice, which gives the symmetric pattern around the first diagonal. Clear density maxima are observed around 1 GeV and around 1.3 GeV in the $\pi^\circ\eta$ system. In the $\pi^\circ\pi^\circ$ system a maximum around 1 GeV seems to appear as well.

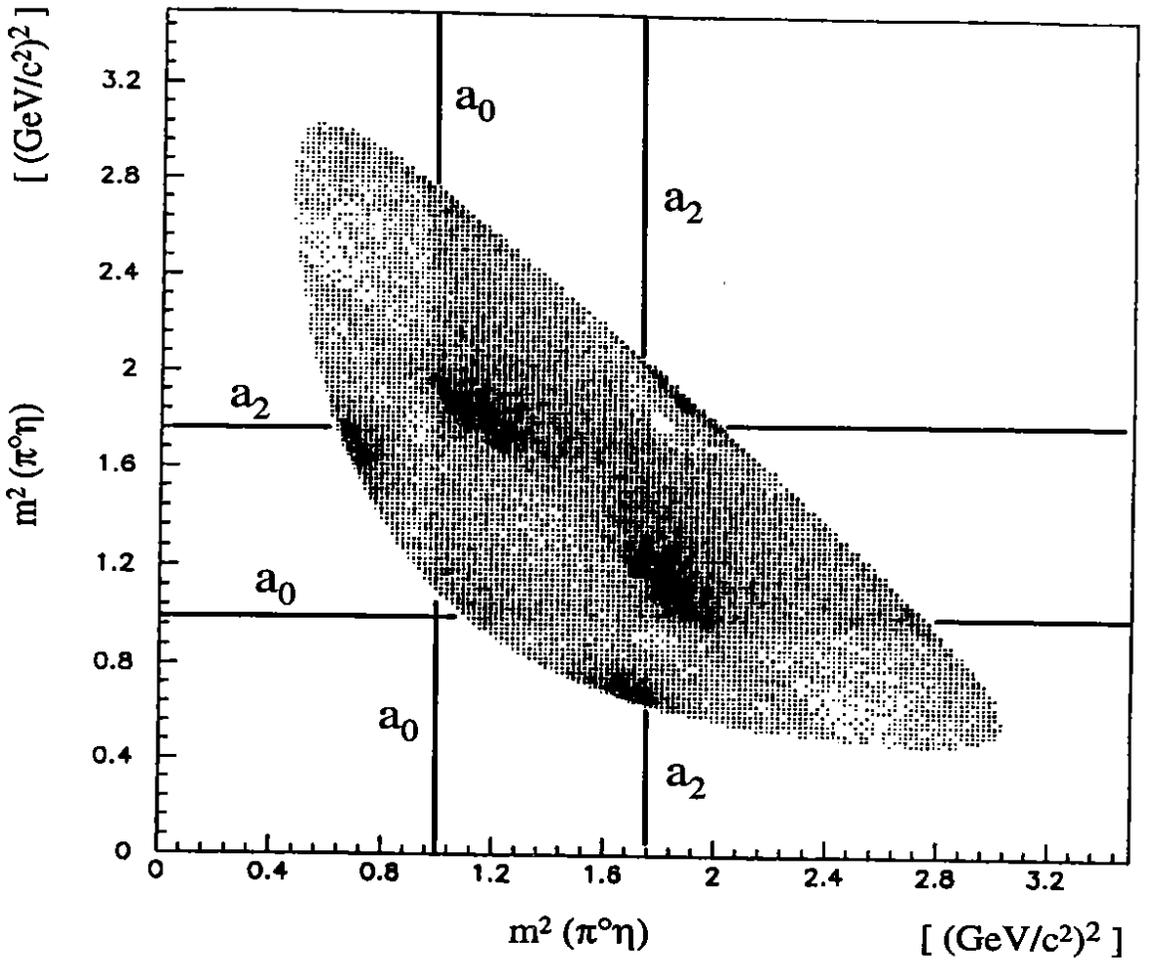

Fig. 7: $\pi^\circ\pi^\circ\eta$ Dalitz plot

The experimental Dalitz plot is reasonably well described with the introduction of at least three amplitudes:

$\bar{p}p \rightarrow \pi^\circ a_0$ with the a_0 (980) decaying $a_0 \rightarrow \pi^\circ\eta$

$\bar{p}p \rightarrow \pi^\circ a_2$ with the a_2 (1320) decaying $a_2 \rightarrow \pi^\circ\eta$

$\bar{p}p \rightarrow \eta f_0$ with the f_0 (975) decaying $f_0 \rightarrow \pi^\circ\pi^\circ$

Strong selection criteria apply to the $\pi^\circ\eta\eta$ Dalitz plot. In this channel, there exists a significant background of $3\pi^\circ$ and $\pi^\circ\pi^\circ\eta$ events. Therefore, only unambiguously identified events enter the Dalitz plot shown in fig. 8. The total number of events in this Dalitz plot is 3,000. Again, each event is plotted twice..

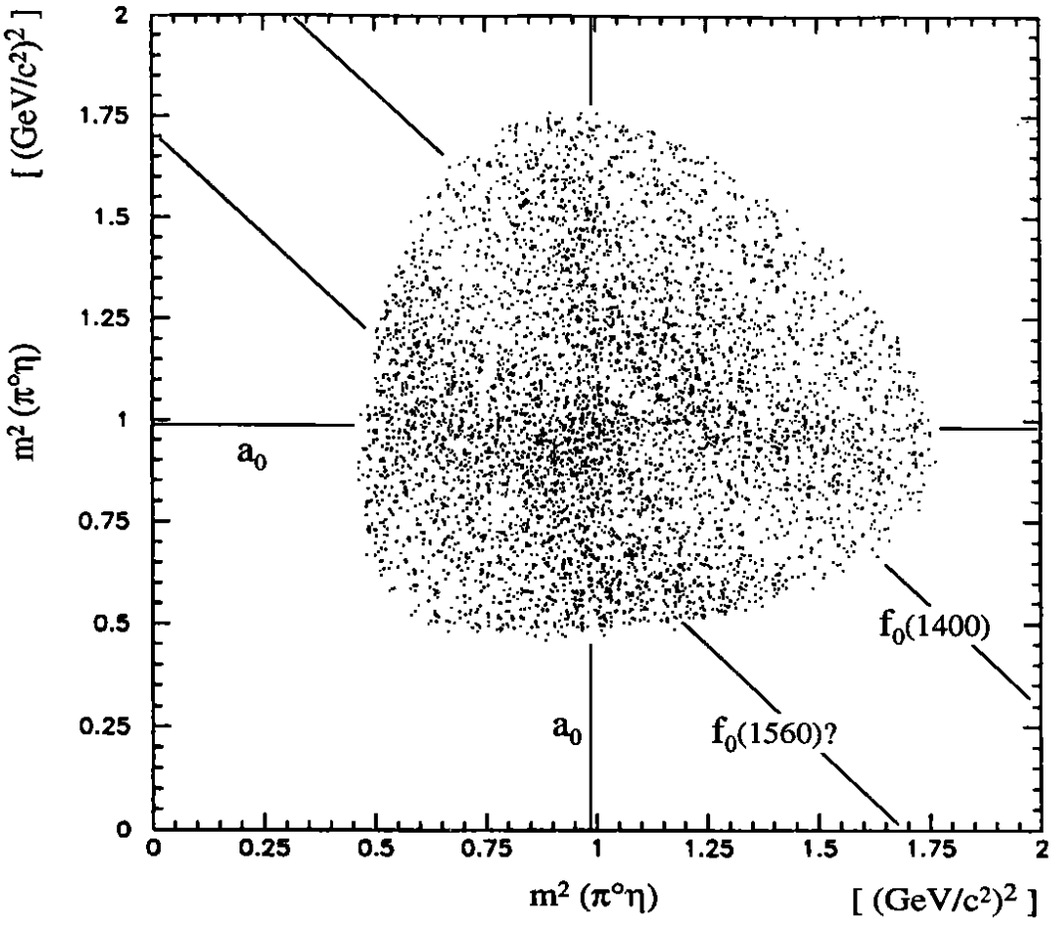

Fig. 8: $\pi^\circ\eta\eta$ Dalitz plot

Density maxima appear in the $\pi^\circ\eta$ mass band around 1 GeV and in the $\eta\eta$ mass band around 1.4 and 1.5 GeV. The best description of the experimental Dalitz plot can be reached by introducing three resonances:

$\bar{p}p \rightarrow \eta a_0$ with the a_0 (980) decaying $a_0 \rightarrow \pi^\circ\eta$

$\bar{p}p \rightarrow \pi^\circ f_0$ with the f_0 (1400) decaying $f_0 \rightarrow \eta\eta$

$\bar{p}p \rightarrow \pi^\circ f_0$ with the f_0 (1560) decaying $f_0 \rightarrow \eta\eta$

The introduction of this new scalar resonance at 1560 MeV is necessary because a fit including the X_2 (1515) fails to describe the data in the $\eta\eta$ mass band around 1.5 GeV. The best fit is achieved using this scalar resonance f_0 (1560) with a width of 200 MeV. More precise values for the description of this Dalitz plot may be achieved with the complete analysis of the Dalitz plot. The scalar meson we observe at 1560 MeV might be identical to the one seen by the GAMS collaboration [8] at 1590 MeV. The GAMS particle is considered a strong glueball candidate.

Tests for strangeness in the nucleon-antinucleon system

If the current picture of hadronic interactions expressed in the theory of Quantum Chromodynamics (QCD) is valid, we should observe the effect of chiral symmetry breaking. The concept of chiral SU(3) symmetry constrains possible effective theories.

The pattern of chiral symmetry breaking, however, does not seem to fit well with the picture that we have in the constituent quark model. The constituent quark model predicts that the proton is composed of solely up and down quarks. To solve the problems connected with chiral SU(3) symmetry breaking, a radical alternative has been suggested in the last years: that the proton contains a sizeable amount of $\bar{s}s$ quarks even at hadronic scales. There are several experimental indications for this hypothesis.

The chiral symmetry breaking operator is measured through the pion-nucleon σ-term. Pion-nucleon scattering data and data with pionic atoms allow for a determination of this π-N-σ-term. Analysis via a standard method [9] yields a nucleon mass that is about 300 MeV too low if the strange quark mass in the proton is set to zero. This result conflicts with the constituent quark model, where the nucleon mass is absolutely independent of the mass of the strange quarks.

The measurements of the European Muon Collaboration (EMC) showed an interesting result [10] that led to the so-called spin crisis of the proton. The EMC used deep inelastic μ-p scattering to determine the amount of spin in the proton carried by each flavour. Not only was the total amount of spin carried by the three light quark flavours practically zero but $\bar{s}s$-pairs were found to carry a significant amount of the proton spin. Both results are in complete disagreement with the constituent quark model; hence the spin crisis.

Meson spectroscopy can be an interesting testing field for the Okubo-Zweig-Iizuka (OZI) rule as well. In the constituent quark model, $\bar{p}p$-annihilation at rest is a reaction containing only up and down quarks in the initial state. The vector mesons mix nearly ideally and the expected deviation from the ideal mixing (calculated with the quadratic Gell-Mann-Okubo mass formula) is **3.7**. The ratio of ω/ϕ-production is therefore expected to be 240 or higher. The measurement of this ratio is considered a crucial test for the validity of the OZI-rule [17].

Early bubble chamber data report a violation of the OZI-rule in the case of ϕ-production in proton proton collisions at 24 GeV/c [11,12]. One experiment, done by the Bombay-CERN-Collège de France-Madrid Collaboration at CERN with the 81 cm Saclay hydrogen bubble chamber, was ded-dedicated to study the ω/ϕ production rate in the channels $\bar{p}p \rightarrow \phi(\omega)\rho^\circ$ and $\bar{p}p \rightarrow \phi(\omega)\pi^+\pi^-$ from 0.7 to 0.76 GeV/c. The conclusion of this experiment is that they see violations of the OZI rule on the order of 5-22%[13]

The ASTERIX experiment belongs to the next generation of experiments at LEAR that did meson spectroscopy in $\bar{p}p$ annihilation at low energies [14, 15] and a detailed study of ω/ϕ branching ratios as seen in $\bar{p}p$ annihilation in hydrogen gas. It found strong OZI-rule violations in the $\phi(\omega)\pi$ system out of s-wave production and little evidence (with limited statistics) in other channels.

OZI-rule violations could be an indication for a strange quark content of the proton. The production of strange mesons is (neglecting non-ideal mixing) only allowed via disconnected diagrams, such as the one in fig. 9.

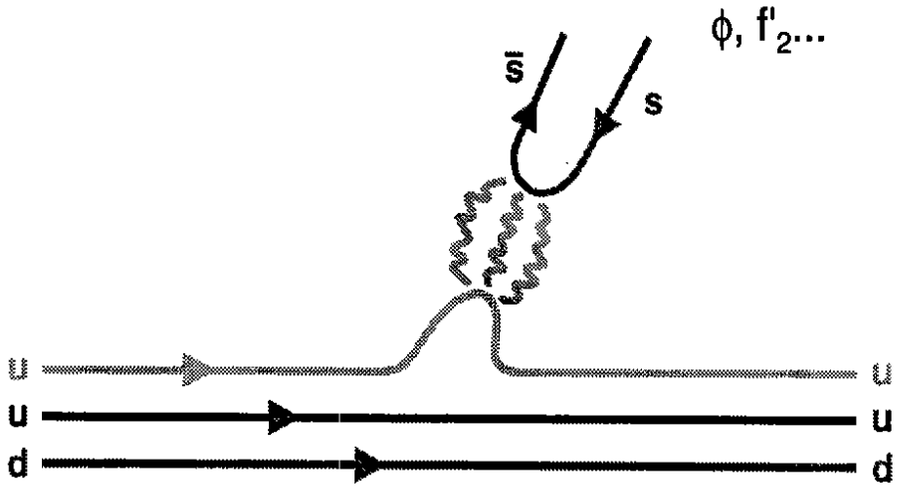

Fig. 9: The coupling of a strange meson to a nonstrange baryon

This is forbidden by the OZI-rule.

One way to evade the OZI rule is to give the proton some amount of strange quark and antiquark pairs (fig. 10).

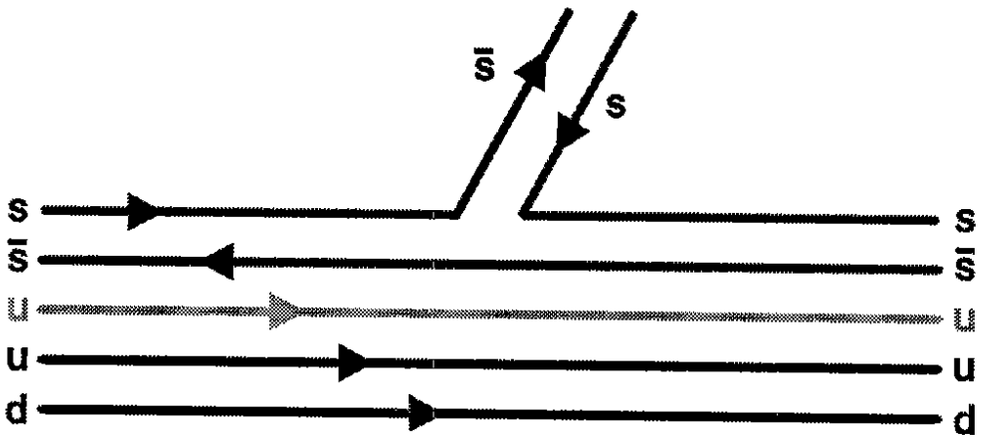

Fig. 10: Coupling of a strange meson to a baryon with strange quark content

The production of mainly ss mesons in pp annihilation would consequently look like the process in fig. 11.

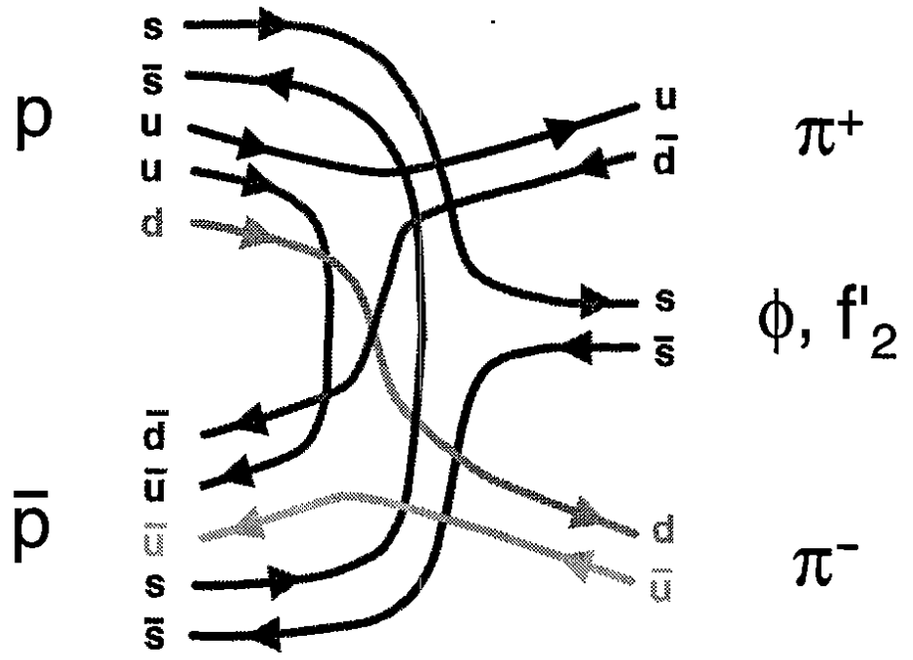

Fig. 11: Production of strange mesons in a $\bar{p}p$ annihilation process

It seems absolutely necessary to improve the data situation with new high precision measurements. The Crystal Barrel experiment is very well suited to do so. We first concentrated on measuring ω/ϕ ratios in $\bar{p}p$ annihilation at rest in liquid hydrogen. The detection of ϕ mesons requires the identification of kaons in the final state. To do so, the dE/dx information of the JDC is helpful in the suppression of pion background. Fig. 12 demonstrates that the dE/dx information allows us to discriminate between pions and kaons up to particle momenta of 400 MeV/c.

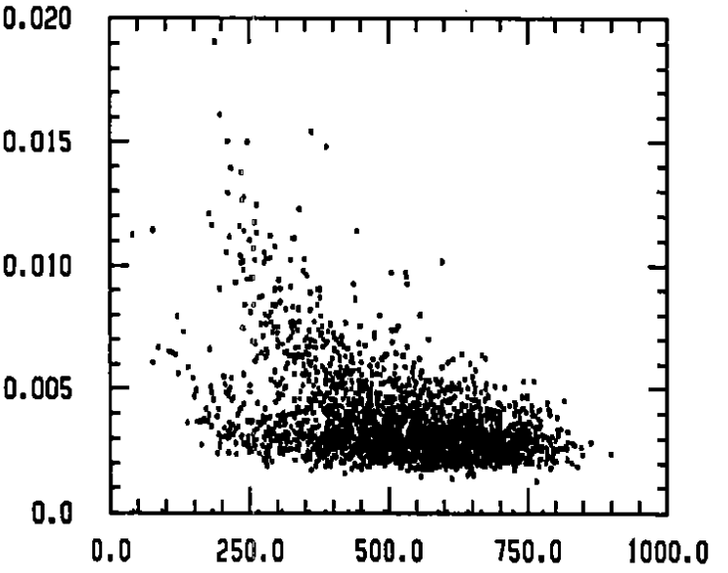

Fig. 12: dE/dx measured with the JDC

ω mesons are detected in the final states $\pi^+\pi^-\pi^\circ\pi^\circ$ and $\pi^+\pi^-\pi^\circ\eta$. The quality of the data is seen in fig. 13 and fig. 14.

The samples of $K^+K^-\pi^\circ$ candidates give a clear ϕ signal in the K^+K^- invariant mass spectrum (fig. 15)

Since no kinematic fitting was applied to this spectrum, the width of the ϕ peak gives an impression of the momentum resolution of the JDC and the quality of the data. The number of ϕ detected (i.e. those decaying into K^+K^-) is between 32 and 43, depending strongly on the description of the background under the ϕ peak. The data analysis for this channel is based on 1 million "minimum-bias" events. The total number of minimum-bias events recorded on tape is so far 10 million.

Another final state that contains ϕ mesons is the channel

$$\bar{p}p \rightarrow K_L K_S \pi^\circ$$

This channel can be selected out of 6γ all-neutral events, if the K_S decays into $2\pi^\circ$. The K_L appears in the missing mass spectrum if it does not interact within the detector.

Fig. 16 shows the Dalitz plot of the channel $\bar{p}p \rightarrow K_L K_S \pi^\circ$ and its projections. The data used have been collected with an all-neutral online trigger. Clear bands of the K^* and a nice sharp band of the ϕ meson appear. The number of ϕ mesons decaying into $K_L K_S$ is determined to be 330. This number is much higher than the observed number of ϕ mesons in minimum-bias data because of the enrichment factor we achieve with an all-neutral trigger. Nevertheless, the normalization of the data for the determination of branching ratios is much more difficult, because the interaction of the K_L particle in the CsI barrel is not very well known.

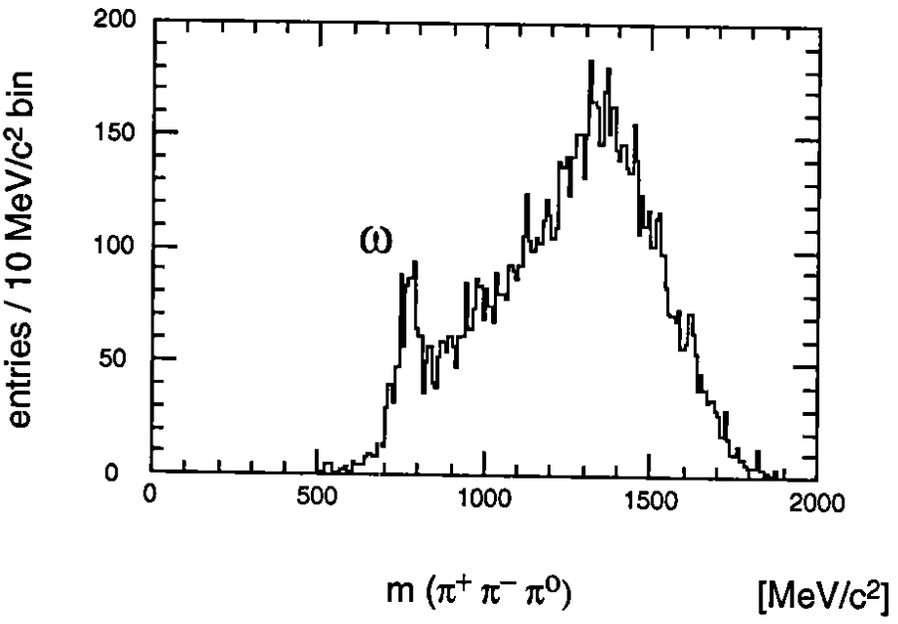

Fig. 13: $\bar{p}p \rightarrow \pi^+\pi^-\pi^\circ\pi^\circ$ final state

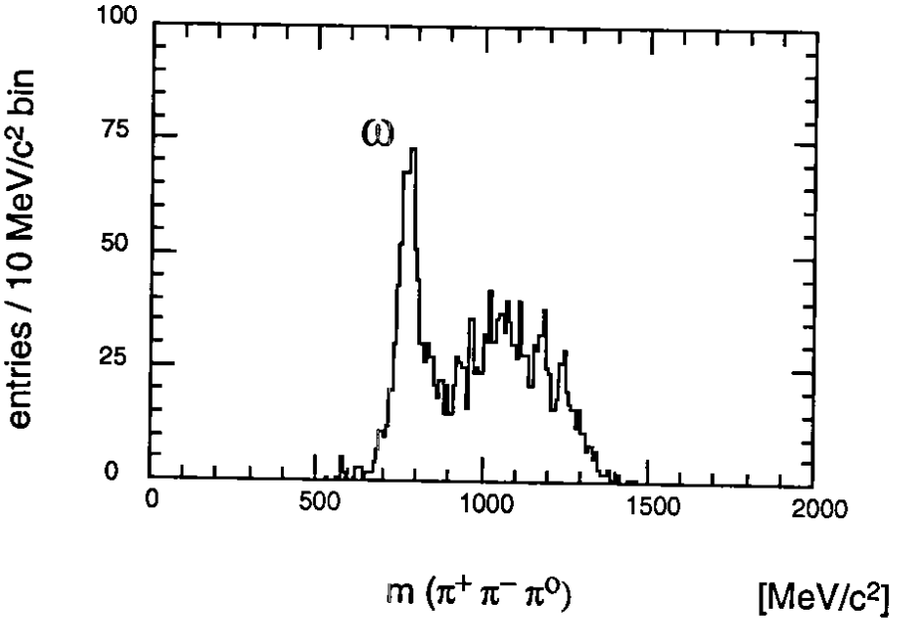

Fig. 14: $\bar{p}p \rightarrow \pi^+\pi^-\pi^\circ\eta$ final state

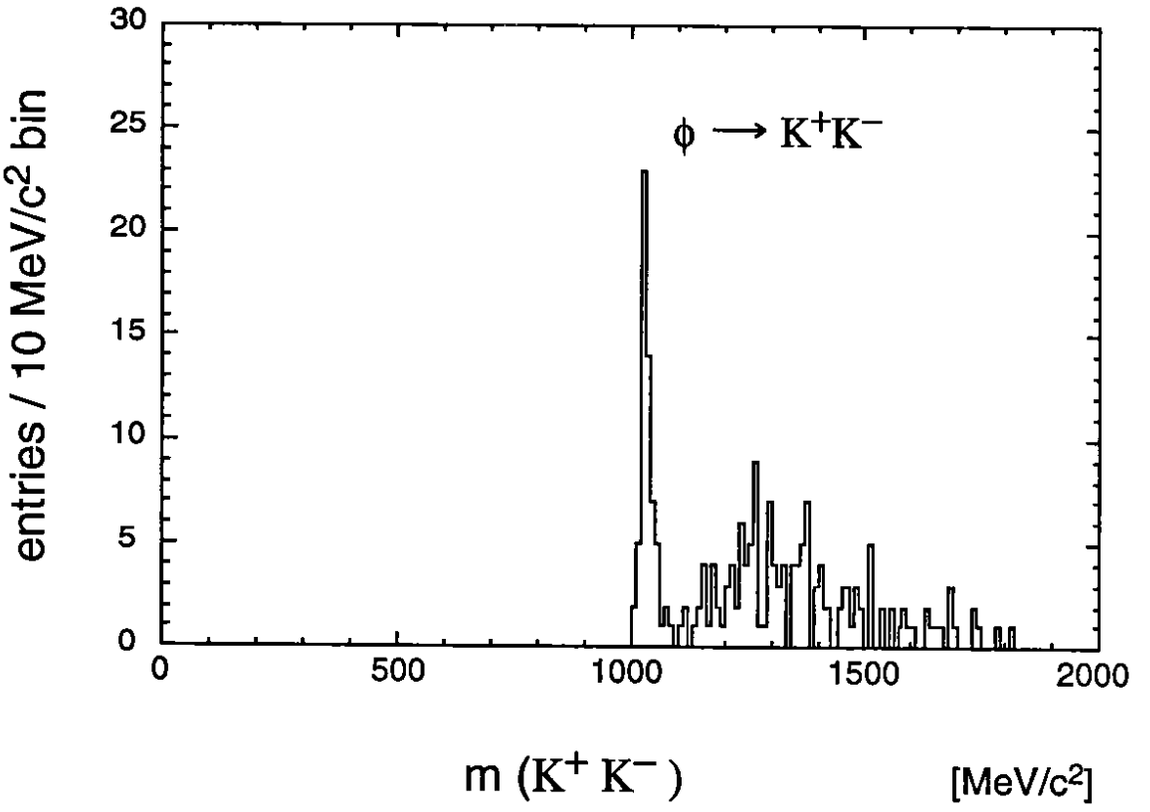

Fig.15: $\bar{p}p \rightarrow K^+K^-\pi^\circ$ final state

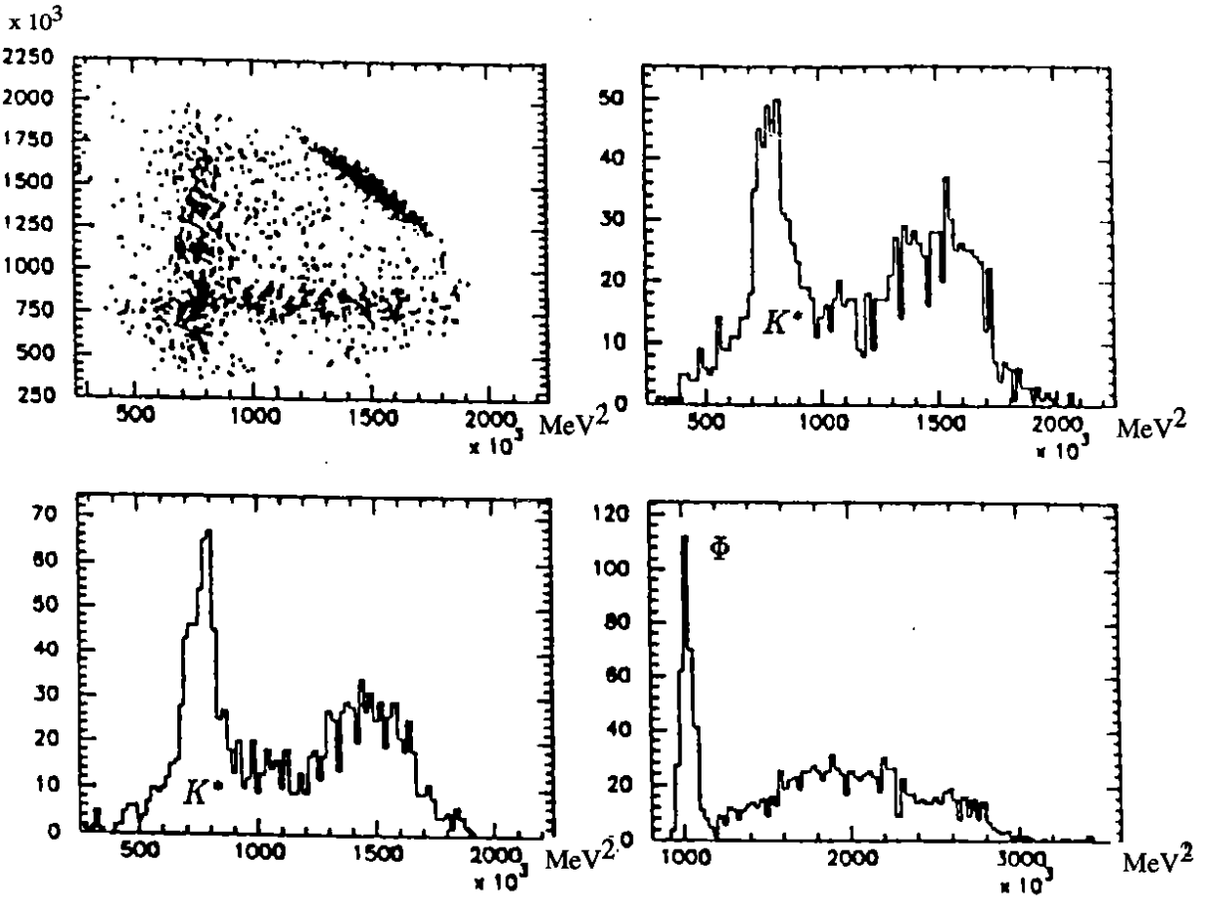

Fig. 16: $pp \rightarrow K_S K_L \pi^\circ$

The following preliminary relative branching ratios were determined (without estimated error) to be:

	Measurements	
	previous	CBAR
$\frac{BR(\bar{p}p \rightarrow \omega\pi^0)}{BR(\bar{p}p \rightarrow \omega\eta)}$	**(0.47-1.13)**	**0.38**
$\frac{BR(\bar{p}p \rightarrow \phi\pi^0)}{BR(\bar{p}p \rightarrow \phi\eta)}$	**(5.14-9.19)**	**(2.56-3.45)**

The evaluation of the interesting branching ratio ϕ/ω is not finished but the preliminary results indicate that we confirm the OZI-rule violations seen by previous experiments.

η Decays as a Test of Low Energy Quantum Chromodynamics

At low energies, the current theory of hadronic interaction reduces to $SU(3)_C \times U(1)_{em}$. Neglecting the mass difference between the up and the down quarks and switching off the electromagnetic interaction conserves isospin and makes the decay $\eta \rightarrow 3\pi$ forbidden by Bose symmetry. The fact that the decay has been observed is consequently only possible due to the quark mass difference m_u-m_d and a contribution of electromagnetic origin. Both terms have been calculated for the decay $\eta \rightarrow 3\pi^\circ$ and for the decay $\eta \rightarrow \pi^+\pi^-\pi^\circ$by Gasser and Leutwyler [16]. Using chiral symmetry, they also give a value for the ratio

$$r = \frac{\Gamma(\eta \rightarrow 3\pi^\circ)}{\Gamma(\eta \rightarrow \pi\pi\pi^\circ)} = 1.44 \pm 0.02$$

A much earlier result of r=1.51 was calculated in the framework of current algebra. In addition, there are six groups that claim experimental results for this ratio. The best of these has an error of +10% and -20% for this value, which is not surprising given that the result is based on a statistic of only 199 events. The Particle Data Group has fitted all given experimental values and has reached a result of r=1.35±0.05. This value disagrees with the theoretical predictions by two to

three standard deviations. The experimental situtation therefore makes it worthwhile to investigate these two decays with a detector that can detect both decay modes of the η with comparable accuracy: the Crystal Barrel detector. It does not seem too ambitous to look for the Dalitz plot distributions of the particles out of the η decay, which is of great interest for chiral symmetry calculations.

The following figures should demonstrate that we are able to achieve this aim. Fig. 17 shows a clear η peak in the final state $\bar{p}p \rightarrow \pi^+\pi^-\pi^\circ\pi^\circ\pi^\circ$

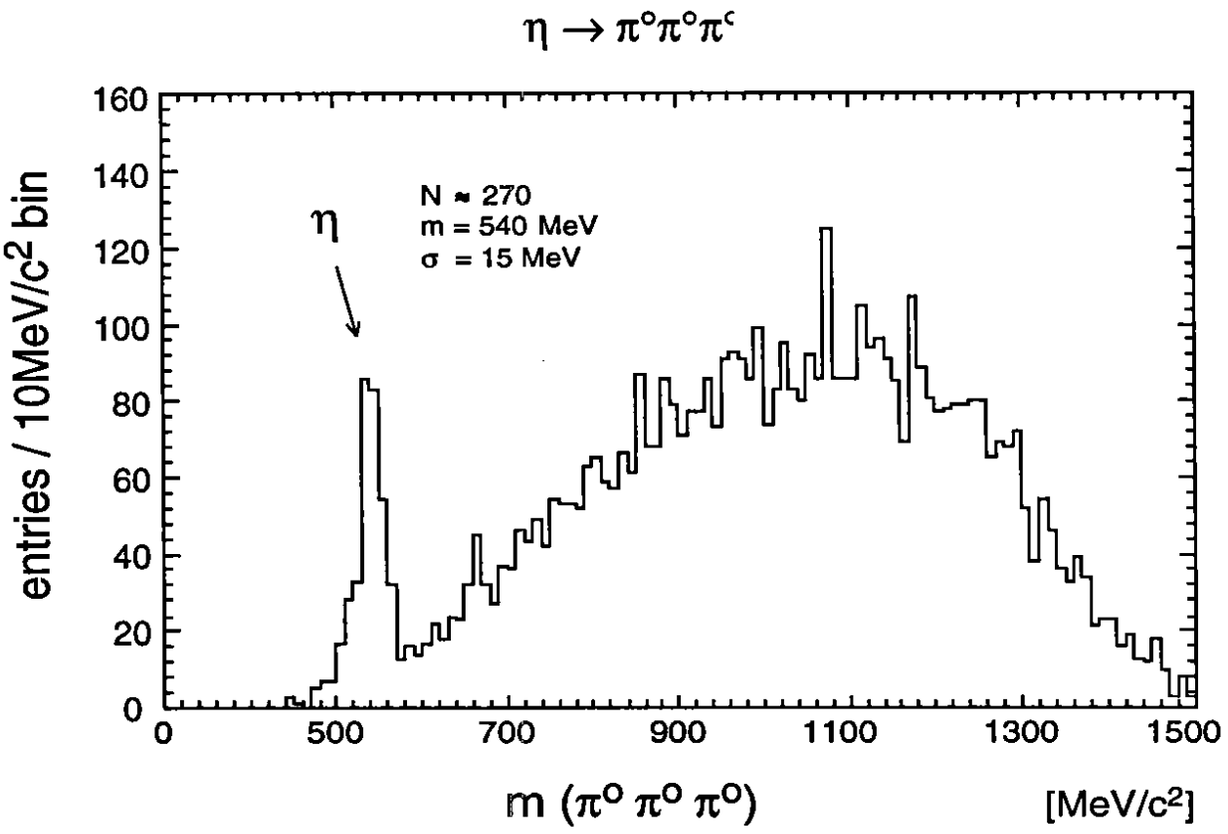

Fig. 17: $\bar{p}p \rightarrow \pi^+\pi^-\pi^\circ\pi^\circ\pi^\circ$

The $\pi^+\pi^-\pi^\circ$ invariant mass spectrum shows as well a signal from the decay $\eta \rightarrow \pi^+\pi^-\pi^\circ$(fig. 18). This signal is not as strong as the one in fig. 17 because of the limited statistics available at the time for this final state. However, ten times the statitics have been taken since then and the analysis is well underway.

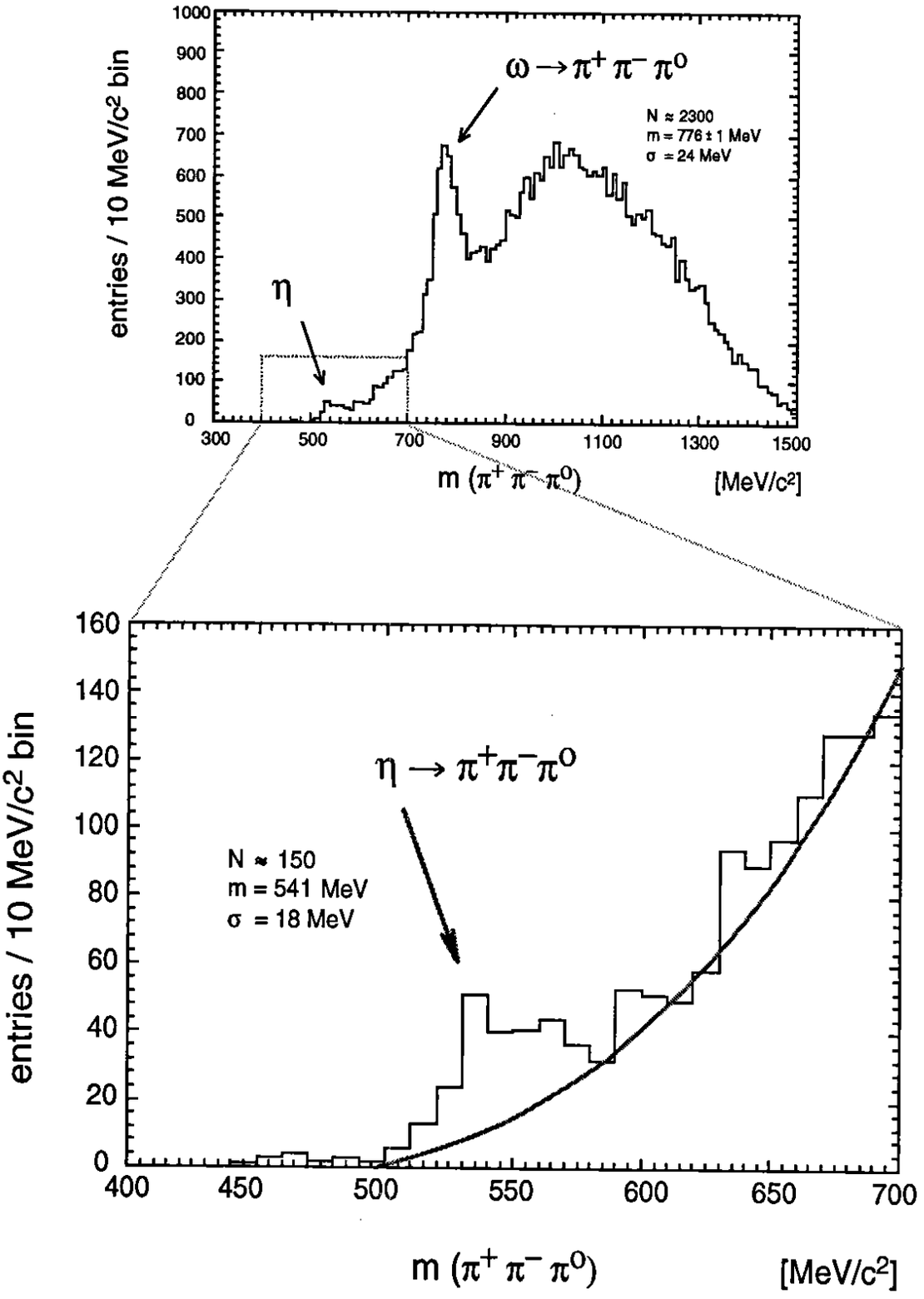

Fig. 18: $\bar{p}p \rightarrow \pi^+\pi^-\pi^+\pi^-\pi^\circ$ final state

Conclusion and Outlook

The Crystal Barrel detector has proven that it is a very efficient all-purpose detector for proton-antiproton annihilations at rest. It can access regions in this field of physics that have never been explored before. In addition, its ability to run selective triggers allows it to search effectively for exotic particles.

It is likely that two new particles have been identified by the Crystal Barrel collaboration so far: the $X_2(1515)$ with $J^{PC}= 2^{++}$ and a scalar meson at 1560 MeV. This scalar meson could be identical with the glueball candidate found by the GAMS collaboration.

Besides the search for new particles, the Crystal Barrel experiment contributes to current questions in medium energy physics, such as that of whether the proton contains strange quarks. Tests of low energy calculations within the chiral pertubation theory are possible by looking at different η decays.

So far only 10-20% of all data taken so far have been analyzed. The results already achieved will therefore improve with increasing statistics. Analysis of data is well underway.

The future plans of the collaboration include extending our measurements to higher energies (i.e. annihilation in flight), to work with a hydrogen gas target, and to measure antiproton annihilation in liquid deuterium.

This work is supported by the German Bundesministerium für Forschung und Technologie, the Schweizerische Nationalfonds, the British Science and Engineering Research Council, and the US Department of Energy.

References

[1] R. Armenteros, B. French, High Energy Physics, Academic Press (Ed. Burhop, E.H.S), 1969
[2] VIII Eur. Symp. Nucleon-Antinucleon Interactions, Thessaloniki, (World Scientific, ed. by S. Charalambous et al.) 1986
[3] R.Veenhof, Program W 5050, CERN program library (1989)
[4] M.Kunze, PhD-Thesis, Karlsruhe 1990 (unpublished)
[5] E. Aker et al.. Phys. Lett. B 260 (1991) 249
[6] B. May et al., Z. Phys. C 46 (1990) 191, C 46 (1990) 203
[7] L.Gray et al., Phys. Rev. D 27 (1983) 307
[8] F. Binon et al., Nuov. Cim. 78 A (1983) 313
[9] J. Gasser, Physics with Light Mesons, Second International Workshop on πN Physics, Los Alamos LA-11184-C (1987)
[10] J. Ashman et al. , Phys. Lett. B 206 (1988) 364, Nucl. Phys. B 328 (1989) 1
[11] V.Blobel et al., DESY preprint 75/31
[12] G. Zweig, CERN-TH 412 (1964); S.Okubo, Phys. Lett. 5 (1965) 1631
[13] A.M. Cooper et al., Nucl. Phys. B 146 (1978) 1
[14] J. Reifenroether et al., Phys. Lett. B 267 (1991) 299
[15] S. Ahmad et al., Nucl. Instr. and Meth. A286 (1990) 76
[16] J. Gasser, H. Leutwyler, Nucl. Phys. B 250 (1985) 539
[17] J. Ellis, E. Gabathuler and M. Karliner, Phys. Lett. B 217 (1989) 173.

Imprimé au CERN. Prix: 0.65 Fr.